https://doi.org/10.46861/bmp.31.041 PŮVODNÍ PRÁCE/ORIGINAL PAPER

Lindgrenite, monoclinic $Cu_3(MoO_4)(OH)_2$, from Cínovec, Krušné hory Mountains - the first occurrence in the Czech Republic

Jiří Sejkora[1)]*, Petr Pauliš[1)2)], Luboš Vrtiška[1)], Ondřej Pour[3)] and Zdeněk Dvořák[4)]

[1)]*Department of Mineralogy and Petrology, National Museum, Cirkusová 1740, 193 00 Praha 9 - Horní Počernice, Czech Republic; *e-mail: jiri.sejkora@nm.cz*
[2)]*Smíškova 564, 284 01 Kutná Hora, Czech Republic*
[3)]*Czech Geological Survey, Geologická 6, 152 00 Praha 5, Czech Republic*
[4)]*Severočeské doly a. s. - doly Bílina, Důlní 375/89, 418 29 Bílina, Czech Republic*

Sejkora J, Pauliš P, Vrtiška V, Pour O, Dvořák Z (2023) Lindgrenite, monoclinic $Cu_3(MoO_4)(OH)_2$, from Cínovec, Krušné hory Mountains - the first occurrence in the Czech Republic. Bull Mineral Petrolog 31(1): 41-46 ISSN 2570-7337

Abstract

A very rare mineral lindgrenite, $Cu_3(MoO_4)_2(OH)_2$, was found in material from the 3rd level of abandoned Cínovec mine 1 of the Cínovec Sn-W deposit, Krušné hory Mountains, northern Bohemia. This is the first occurrence of this mineral in the Czech Republic. Lindgrenite occurs there as olive green irregular coatings on the area up to 0.5 × 1 cm in size formed by hemispherical to spherical aggregates up to 0.3 mm across with crystalline surface in association with brochantite. Lindgrenite is monoclinic, space group $P2_1/n$, the unit-cell parameters refined from X-ray powder diffraction data are: *a* 5.3934(18), *b* 14.032(2), *c* 5.6098(15) Å, *β* 98.54(2)° and *V* 419.86(16) Å^3. Chemical analyses of lindgrenite correspond to the empirical formula $(Cu_{2.92}Fe_{0.03})_{\Sigma 2.95}(MoO_4)_{1.97}(PO_4)_{0.07}(AsO_4)_{0.01}(OH)_{1.70}$ on the basis of 5 atoms *pfu*. Its origin is connected with simultaneous weathering of primary Cu (tennantite) and Mo (molybdenite) minerals in the conditions of supergene zone *in-situ*.

Key words: *lindgrenite, unit-cell parameters, chemical composition, Raman spectroscopy, Cínovec, Czech Republic*

Received 3. 4. 2023; accepted 16. 6. 2023

Introduction

Copper molybdates, lindgrenite $Cu_3(MoO_4)_2(OH)_2$, szenicsite $Cu_3(MoO_4)(OH)_4$, markascherite $Cu_3(MoO_4)(OH)_4$, cupromolybdite $Cu_3O(MoO_4)_2$ and huenite $Cu_4(MoO_4)_3(OH)_2$ are representing rare supergene minerals formed by simultaneous weathering of primary Cu sulfides and molybdenite or as a product of fumarolic activity (cupromolybdite). Lindgrenite was originally described as a new mineral species from the great porphyry copper deposit at Chuquicamata, Chile by Palache (1935). Later, it was found at other localities in Chile, France, Japan, Morocco, Norway and USA (https://www.mindat.org/min-2405.html) but its occurrence in the Czech Republic was not known yet. Synthetic analogues of lindgrenite with 0D to 3D architecture (rods, plates, urchin-like structures, nanoflowers or hollow spheres) has attracted strong interest due to their promising applications in various technological fields, such as photocatalysts, electrical conductivity, magnetism, photochemistry, solid-state electrolytes, sensors, organic-inorganic hybrid materials and energy storage (e.g. Moini et al. 1986; Shores et al. 2005; Vilminot et al. 2006; Xu, Xue 2007; Shahri et al. 2014; Swain et al. 2017; Martins et al. 2018 and others).

Occurrence and specimen description

Lindgrenite was found on specimens originating from the Cínovec Sn-W deposit, located approximately 15 km N of Teplice, Krušné hory Mountains, Czech Republic. The studied samples were found in January 2022 at abandoned stope at the 3rd level of Cínovec mine (Militärschacht). The „classic“ Cínovec vein-type deposit is situated in apical part of elevation of lithium albite granite, which formed at surface irregular ellipsis with dimensions 300 x 1400 m. This vein deposit is represented by system of 13 subhorizontal veins, which are accompained by lateral greisenization (Pauliš et al. 2022). It belongs to the richest (65 primary and 58 supergene mineral species) and most interesting mineralogical localities in the Czech Republic (Pauliš et al. 2022).

Studied samples are represented by massive white to smoky colored quartz gangue with rare and tiny molybdenite flakes in intergranulars and aggregates of tennantite, cassiterite and *zinnwaldite* up to 3 cm in size. Tennantite aggregates are partly supergene altered to form flat vugs up to 1.5 cm in length. Lindgrenite occurs in these vugs as irregular coatings (Fig. 1) on the area up to 0.5 × 1 cm in size. Its coatings are formed by hemispherical to spherical aggregates up to 0.3 mm across (Fig. 2) with crystalline surface (individul prismatic crystals only 5 - 10 μm in size). Lindgrenite is olive green with vitreous lustre, very brittle, translucent only in tiny fragments. Light to dark green aggregates of brochantite up to 1 mm size were observed in association with lindgrenite.

Chemical composition

Samples of lindgrenite were analysed with a Cameca SX-100 electron microprobe (National Museum, Prague) operating in the wavelength-dispersive mode with an accelerating voltage of 15 kV, a specimen current of 5 nA, and a beam diameter of 20 μm. The following lines and standards

Fig. 1 *Olive green crystalline aggregate of lindgrenite in small vugs of supergene altered tennantite from Cínovec; field of view 5.8 mm; photo B. Bureš.*

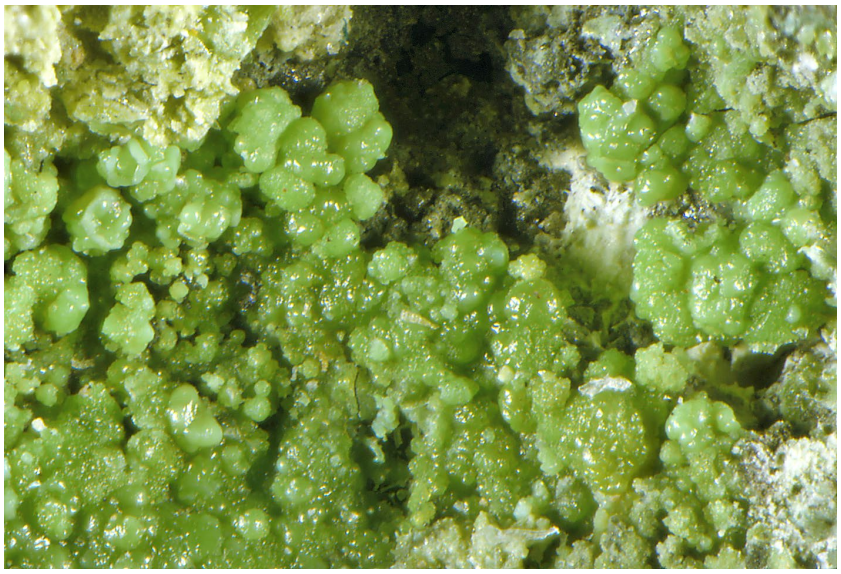

Fig. 2 *Olive green hemispherical aggregates of lindgrenite from Cínovec; field of view 2.6 mm; photo J. Sejkora.*

were used: *K*α: chalcopyrite (Cu), hematite (Fe), fluorapatite (P) and *L*α: clinoclase (As), wulfenite (Mo). Peak counting times (CT) were 20 s; CT for each background was one-half of the peak time. The raw intensities were converted to the concentrations automatically the using *PAP* (Pouchou and Pichoir 1985) matrix-correction algorithm. Water content could not be analysed directly because of the minute amount of material available. The H_2O content (presence of OH groups) was confirmed by Raman spectroscopy and calculated by charge balance.

Chemical composition of lindgrenite sample (Table 1) agrees with ideal formula $Cu_3(MoO_4)_2(OH)_2$. The cationic sites are occupied by dominant Cu with only minor contents of Fe up to 0.05 *apfu*. The anion site is dominated by Mo and only partly substituted by P and As up to 0.08 and 0.02 *apfu*, respectively. The empirical formula of studied lindgrenite (mean of 9 analyses) calculated on the basis of 5 atoms *pfu* is following: $(Cu_{2.92}Fe_{0.03})_{\Sigma 2.95}(MoO_4)_{1.97}(PO_4)_{0.07}(AsO_4)_{0.01}(OH)_{1.70}$.

X-ray powder diffraction

Powder X-ray diffraction data were collected on a Bruker D8 Advance diffractometer (National Museum, Prague) with a solid-state 1D LynxEye detector using CuK_α radiation and operating at 40 kV and 40 mA. The powder pattern was collected using Bragg–Brentano geometry in the range 2.5 - 70° 2θ, in 0.01° steps with a counting time of 20 s per step. Positions and intensities of reflections were found and refined using the Pearson VII profile-shape

Table 1 *Chemical composition of lindgrenite from Cínovec (wt. %)*

	mean	1	2	3	4	5	6	7	8	9
FeO	0.40	0.62	0.34	0.45	0.22	0.39	0.40	0.29	0.51	0.39
CuO	42.56	41.29	42.59	42.38	43.40	42.29	42.48	42.93	42.29	43.39
MoO_3	52.17	50.76	52.06	52.14	52.37	52.92	52.29	52.44	52.57	51.99
As_2O_5	0.27	0.38	0.07	0.47	0.23	0.00	0.18	0.48	0.22	0.36
P_2O_5	0.87	0.88	0.90	0.71	0.86	0.90	0.99	0.87	0.97	0.76
H_2O*	2.82	2.73	2.86	2.80	2.95	2.71	2.76	2.79	2.70	3.04
total	99.08	96.66	98.82	98.95	100.03	99.21	99.10	99.80	99.26	99.93
Fe	0.030	0.048	0.026	0.034	0.017	0.030	0.030	0.022	0.039	0.029
Cu	2.915	2.896	2.925	2.910	2.944	2.898	2.907	2.919	2.891	2.946
Mo	1.975	1.968	1.976	1.979	1.963	2.004	1.978	1.970	1.986	1.950
As	0.013	0.018	0.003	0.022	0.011	0.000	0.009	0.023	0.010	0.017
P	0.067	0.069	0.069	0.055	0.065	0.069	0.076	0.066	0.074	0.058
OH	1.703	1.691	1.732	1.701	1.766	1.639	1.666	1.674	1.633	1.825

Mean of 9 point analyses; 1-9 point analyses; *apfu* on the base Fe+Cu+Mo+As+P = 5; H_2O* calculated on the base of charge balance

function with the ZDS program package (Ondruš 1993) and the unit-cell parameters were refined by the least-squares algorithm implemented by Burnham (1962). The experimental powder pattern was indexed in line with the calculated values of intensities obtained from the crystal structure of lindgrenite (Hawthorne, Eby 1985), based on Lazy Pulverix program (Yvon et al. 1977).

The peak positions in experimental X-ray powder pattern (Table 2) agree well with published data for lindgrenite as well as with those calculated from the crystal structure of this mineral (Hawthorne, Eby 1985). The observed differences in intensities of individual diffraction maxima are caused by preferred orientation effects due to {010} perfect cleavage. The refined unit-cell parameters are compared in the Table 3 with published data.

Raman spectroscopy

The Raman spectra of studied sample were collected in the range 4000 - 30 cm^{-1} using a DXR dispersive Raman Spectrometer (Thermo Scientific) mounted on a confocal Olympus microscope. The Raman signal was excited by an unpolarised green 532 nm solid state, diode-pumped laser and detected by a CCD detector. The experimental parameters were: 100x objective, 5 s exposure time, 500 exposures, 50 μm slit spectrograph aperture and 2 mW laser power level. The spectra were repeatedly acquired from different grains in order to obtain a representative spectrum with the best signal-to-noise ratio. The eventual thermal damage of the measured point was excluded by visual inspection of excited surface after measurement,

Table 2 *X-ray powder diffraction data of lindgrenite from Cínovec*

d_{obs}	I_{obs}	d_{calc}	h	k	l	d_{obs}	I_{obs}	d_{calc}	h	k	l	d_{obs}	I_{obs}	d_{calc}	h	k	l
7.019	29	7.016	0	2	0	2.722	4	2.721	0	1	2	1.9358	2	1.9372	1	4	2
4.355	9	4.352	0	2	1	2.684	16	2.684	-1	4	1	1.9086	1	1.9089	2	4	1
4.165	30	4.166	-1	0	1	2.668	10	2.667	2	0	0	1.8861	8	1.8853	0	7	1
3.582	13	3.588	1	0	1	2.516	6	2.515	-2	1	1	1.8764	6	1.8765	1	7	0
		3.582	-1	2	1	2.507	8	2.504	0	5	1	1.7591	3	1.7583	2	6	0
3.511	100	3.517	1	3	0	2.4604	4	2.4592	-1	2	2	1.7531	4	1.7541	0	8	0
		3.508	0	4	0	2.4025	7	2.4019	-2	2	1	1.7188	4	1.7197	0	3	3
3.477	27	3.476	1	1	1	2.3365	3	2.3387	0	6	0	1.6661	4	1.6663	1	8	0
2.964	4	2.965	0	4	1	2.2952	5	2.2924	1	1	2	1.5968	3	1.5972	2	4	2
2.931	2	2.931	1	4	0	2.2109	4	2.2105	1	5	1	1.5942	2	1.5949	-2	2	3
2.849	4	2.847	1	3	1	2.1558	2	2.1551	0	6	1	1.5767	3	1.5775	-2	7	1
2.775	6	2.774	0	0	2	2.0840	2	2.0832	-2	0	2	1.4972	6	1.4965	1	9	0

Table 3 *Unit-cell parameters for lindgrenite (for monoclinic space group $P2_1/n$)*

		a [Å]	b [Å]	c [Å]	β [°]	V [Å^3]
Cínovec	this paper	5.3934(18)	14.032(2)	5.6098(15)	98.54(2)	419.86(16)
Chuquicamata	Hawthorne, Eby (1985)	5.394	14.023	5.608	98.50	419.53
synth.	Bao et al. (2006)	5.3867(10)	14.001(3)	5.6010(11)	98.535(2)	417.73(14)
Chuquicamata	Barnes (1949a,b)	5.405	14.03	5.613	98.38	420.49
Sansei	Miyazaki et al. (2002)	5.401(1)	14.043(2)	5.620(1)	98.49(1)	421.58

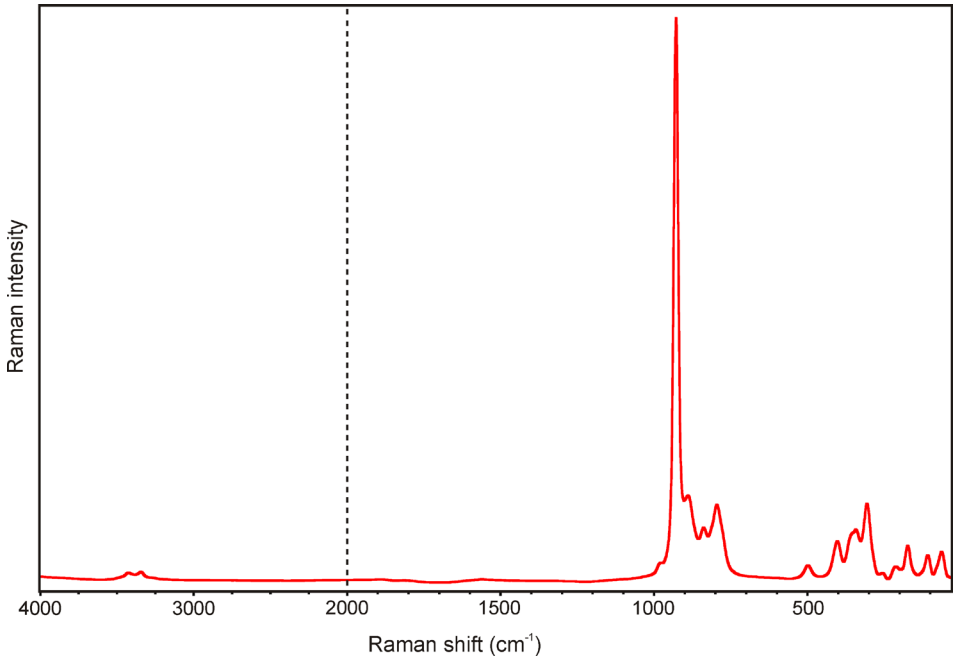

Fig. 3 *Raman spectrum for lindgrenite from Cínovec (split at 2000 cm^{-1}).*

Table 4 *Tentative assignment of Raman spectrum of lindgrenite from Cínovec*

position	*FWHH*	$I_{rel.}$	$I_{rel.}$	*position*		*tentative assignment*
[cm^{-1}]	[cm^{-1}]	height	area	1*	2*	
3425	68	1.2	7.2			
3385	40	0.3	0.6			ν OH stretch of OH groups
3342	41	1.1	2.8			
3273	122	0.3	2.3			
980	17	1.2	1.2	982		
928	17	100.0	100.0	929	932	ν_1 symmetric stretch of $(MoO_4)^{2-}$
887	38	12.3	27.5	883	887	
838	30	6.8	12.0	837	839	
798	30	11.1	19.4	795	798	ν_3 antisymmetric stretch of $(MoO_4)^{2-}$
778	21	4.8	5.7	772	772	
498	29	2.4	4.2	493	496	stretch of Cu-O bonds
403	30	6.7	12.5	398	399	ν_2 bend of $(MoO_4)^{2-}$
361	24	5.4	7.0	354	342	
340	26	6.7	9.7	335	335	ν_4 bend of $(MoO_4)^{2-}$
305	29	13.3	23.2	300	302	
253	15	0.9	0.8		251	
212	27	2.3	3.2	210	217	
173	22	6.3	9.4	167	171	Cu-O interactions, rotational or translational modes of $(MoO_4)^{2-}$ group, lattice modes.
108	20	4.3	6.0			
78	11	0.9	0.5			
62	20	4.7	4.6			

$I_{rel.}$ calculated from peak height and band area; 1* lindgrenite from Pinal Co, USA (G16506); 2* lindgrenite from Broken Hill, Australia (M21019); both data from Frost et al. (2004).

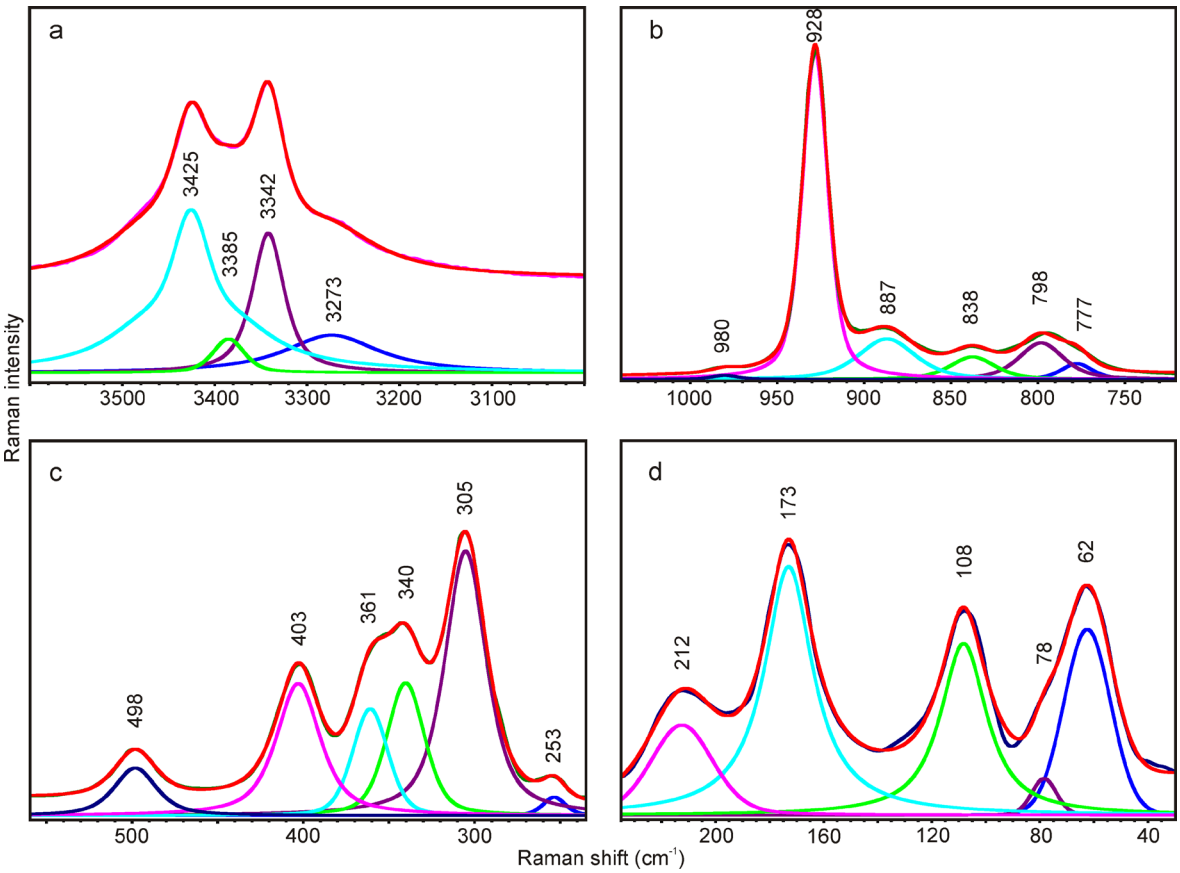

Fig. 4 *Results of the band component analysis in the Raman spectrum of lindgrenite from Cínovec: a) 3600 - 3000 cm^{-1}; b) 1040 - 720 cm^{-1}; c) 560 - 235 cm^{-1}; d) 235 - 30 cm^{-1}.*

by observation of possible decay of spectral features in the start of excitation and checking for thermal downshift of Raman lines. The instrument was set up by a software-controlled calibration procedure using multiple neon emission lines (wavelength calibration), multiple polystyrene Raman bands (laser-frequency calibration) and standardized white-light sources (intensity calibration).

Spectral manipulations were performed using the Omnic 9 software (Thermo Scientific). Gaussian/Lorentzian (pseudo-Voigt) profile functions of the band-shape were used to obtain decomposed band components of the spectra. The decomposition was based on the minimization of the difference in the observed and calculated profiles until the squared correlation coefficient (r^2) was greater than 0.995.

Lindgrenite, $Cu_3(MoO_4)_2(OH)_2$, is a monoclinic hydroxyl copper molybdate, the space group $P2_1/n$, $Z = 2$. In the asymmetric part of the unit-cell, there are two pseudo-octahedrally coordinated Cu cations and one Mo site coordinated by four oxygens in tetrahedral arrangement with significant differences in individual Mo-O bonds (1.743 - 1.749 and 1.774 - 1.779 Å, respectively). The crystal structure consists of strips of edge-sharing $CuØ_6$ (Ø - unspecified ligand) octahedra that are cross-linked by MoO_4 tetrahedra. Alternate strips are canted at ± 25° to (100), the sense of the tilt being along Y. This results in close-packed layers parallel to (100) (Hawthorne, Eby 1985).

Free $(MoO_4)^{2-}$ tetrahedra exhibits *T*d tetrahedral symmetry. In the case of the free anion of *T*d symmetry, there may be theoretically observed nine normal vibrations ν_1 (A_1) symmetrically stretching vibration, Raman active, 897 (1100 - 850) cm^{-1}, ν_2 (E) doubly degenerate bending vibrations, Raman active, 315 (500 - 300) cm^{-1}, ν_3 (F_2) triply degenerate antisymmetric stretching vibrations, Raman and infrared active, 837 (820 - 720) cm^{-1}, ν_4 (F_2) triply degenerate bending vibrations, Raman and infrared active, 315 (500 - 300) cm^{-1} (Nakamoto 2009; range by Saraf et al. 2010 are given in parentheses). *T*d symmetry lowering may cause splitting of degenerate vibrations and Raman and infrared activation of all vibrations depending on the symmetry of $(MoO_4)^{2-}$ units. Wavenumbers of the ν_1 $(MoO_4)^{2-}$ symmetric stretching vibrations are higher than the ν_3 $(MoO_4)^{2-}$ antisymmetric vibrations thus differing e.g. with $(SO_4)^{2-}$, possessing the same *T*d symmetry. This fact is generally accepted, however, no unity may be observed for the $(MoO_4)^{2-}$ bending vibrations. The ν_2 $(MoO_4)^{2-}$ bending vibrations are therefore assigned in some papers to higher wavenumbers than the ν_4 $(MoO_4)^{2-}$ and in some other papers vice versa or do not distinguish between these two vibrations (Sejkora et al. 2014).

Hydroxyl ions, $(OH)^-$, (point symmetry $C_{\infty v}$) are commonly indicated by sharp bands between 3700 and 3450 cm^{-1}, but sometimes at lower wavenumbers, if any appreciable amount of hydrogen bonding is involved, δ M-OH approximately at 1500 cm^{-1} and over wide range below this value, and OH^- libration modes in the spectra range from 1000 to 300 cm^{-1} (Lutz 1995). According to Nakamoto (2009), octahedral units XY_6 (O_h) exhibit six normal vibrations: ν_1 (A_{1g}) and ν_2 (E_g) stretching and ν_5 (F_{2g}) bending vibrations are Raman active, while only ν_3 (F_{1u}) stretching and ν_4 (F_{1u}) bending vibrations are infrared active. The ν_6 (F_{2u}) bending vibrations are neither Raman nor infrared active. Symmetry lowering in the case of $XY_{6-x}Z_x$ may cause Raman and infrared activation of corresponding vibrations and splitting of degenerate vibrations. Cu-O stretching and bending vibrations are usually located in the region approximately from 360 to 600 cm^{-1}.

The Raman spectrum of lindgrenite from Cínovec is close to the published spectra of this mineral from Pinal Co, USA and Broken Hill, Australia (Frost et al. 2004) and corresponds also very well with Raman spectra of synthetic $Cu_3(MoO_4)_2(OH)_2$, studied in detail by Martins et al. (2018). The experimental full-range Raman spectrum of the lindgrenite from Cínovec is given in Figure 3 and wavenumbers with tentative assignments are given in Table 4. Bands of the very low intensity in region 3500 - 3200 cm^{-1} with components at 3425, 3385, 3342 and 3273 cm^{-1} (Fig. 4a) are attributed to the ν OH stretching vibrations of OH groups. According to the empirical relation between energy of vibration and the corresponding bond length (Libowitzky 1999), O-H×××O hydrogen-bond lengths vary approximately in the range from 2.73 to 2.82 Å, which are consistent with value 2.81 Å derived from crystal structure refinement (Hawthorne, Eby 1985).

Very strong band at 928 cm^{-1} with shoulders at 980 and 887 cm^{-1} (Fig. 4b) is assigned to the ν_1 $(MoO_4)^{2-}$ symmetric stretching vibration, presence of three components of this vibration probably reflects different Mo-O lengths in MoO_4 tetrahedra; similar character of this part of spectra was observed also for synthetic $Cu_3(MoO_4)_2(OH)_2$ - very strong band at 932 cm^{-1} with shoulders at 987, 902 and 888 cm^{-1} (Martins et al. 2018). Three medium-strong bands at 838, 798 and 778 cm^{-1} (Fig. 4b) are connected with ν_3 triply degenerate antisymmetric stretching vibrations of $(MoO_4)^{2-}$ group and weak those at 498 cm^{-1} probably with stretching vibrations of Cu-O bonds of $CuØ_6$ octahedra. Medium-strong band at 403 cm^{-1} is attributed to ν_2 doubly degenerate bending vibrations and bands at 361, 340 and 305 cm^{-1} (Fig. 4c) to ν_4 triply degenerate bending vibrations of $(MoO_4)^{2-}$ group. As mentioned above, the assignment of ν_2 and ν_4 vibrations is not unambiguous. Raman bands at 253, 212, 173, 108, 78 and 62 cm^{-1} (Fig. 4d) are associated with Cu-O interactions, rotational or translational modes of $(MoO_4)^{2-}$ group, as well as the lattice modes.

Conclusion

Very rare mineral, lindgrenite, was determined in the material from the Cínovec Sn-W deposit (Czech Republic) by X-ray powder diffraction and electron microprobe analyses. Molecular structure of this well-defined sample can be better constrained using the Raman spectroscopy which confirmed the presence of hydroxyl groups and molybdate units in its crystal structure. This is the first occurrence of this mineral in the Czech Republic. Its origin is connected with simultaneous weathering of primary Cu (tennantite) and Mo (molybdenite) minerals in the conditions of supergene zone *in-situ*.

Acknowledgements

The study was financially supported by the Ministry of Culture of the Czech Republic (long-term project DKRVO 2019-2023/1.II.e; National Museum, 00023272). The authors thank to Milan Svitek (Osek) who kindly provided sample for study and to Bohuslav Bureš (Prague) for photo.

References

Bao RL, Kong ZP, Min GU, Bin YUE, Weng LH, He HY (2006) Hydrothermal synthesis and thermal stability of natural mineral lindgrenite. Chemical Research in Chinese Universities, 22(6): 679-683

Barnes WH (1949a) Corrections to recent papers on probertite and lindgrenite. Am Mineral 34(7-8): 611-613

Barnes WH (1949b) The unit cell and space group of lindgrenite. Am Mineral 34(3-4): 163-172

Burnham Ch W (1962) Lattice constant refinement. Carnegie Inst Washington Year Book 61: 132-135

Frost R, Duong L, Weier M (2004) Raman microscopy of the molybdate minerals koechlinite, iriginite and lindgrenite. N Jb Mineral, Abh 180(3): 245-260

Hawthorne FC, Eby RK (1985) Refinement of the crystal structure of lindgrenite. N Jb Mineral, Mh 1985(5): 234-240

Libowitzky E (1999) Correlation of O-H stretching frequencies and O-H×××O hydrogen bond lengths in minerals. Monat Chem 130: 1047-1059

Lutz HD (1995) Hydroxide ions in condensed materials - correlation of spectroscopic and structural data. *In:* Alcock NW, ed. Structure and bonding Vol. 82 Coordination chemistry p. 86-103, Springer Verlag, Berlin Heidelberg

Martins GM, Coelho PO, Moreira RL, Dias A (2018) Hydrothermal synthesis and polarized micro-Raman spectroscopy of copper molybdates. Ceramics Internat 44(11): 12426-12434

Miyazaki I, Ohori S, Kishi S, Kobayashi S, Kusachi I (2002) Lindgrenite from the Sansei mine, Nara Prefecture, Japan. J Mineral Petrolog Sci 97(4): 207-210

Moini A, Peascoe R, Rudolf PR, Clearfield A (1986) Hydrothermal synthesis of copper molybdates. Inorg Chem 25(21): 3782-3785

Nakamoto K (2009) Infrared and Raman spectra of inorganic and coordination compounds Part A Theory and applications in inorganic chemistry. John Wiley and Sons Inc. Hoboken, New Jersey

Ondruš P (1993) ZDS - A computer program for analysis of X-ray powder diffraction patterns. Materials Science Forum, 133-136, 297-300, EPDIC-2. Enchede.

Palache C (1935) Lindgrenite, a new mineral. Am Mineral 20(7): 484-491

Pauliš P, Dvořák Z, Babka K, Fuchs P (2022) Nerostné bohatství Krupky, Cínovce a Moldavy. Kuttna, Kutná Hora.

Pouchou J, Pichoir F (1985) „PAP“ (φρz) procedure for improved quantitative microanalysis. In: Armstrong JT (ed): Microbeam Analysis: 104-106. San Francisco Press. San Francisco

Saraf U, Bajpai PK, Chowdhury RNP (2010) Vibrational Raman and FTIR studies of some double alkali molybdates/tungstates. J Int Acad Phys Sci 14(1): 81-90

Sejkora J, Čejka J, Malíková R, López A, Xi Y, Frost RL (2014) A Raman spectroscopic study of a hydrated molybdate mineral ferrimolybdite, $Fe_2(MoO_4)_3 \cdot 7\text{-}8\ H_2O$. Spectrochim Acta A: Molec Biomolec Spectrosc 130: 83-89

Shahri Z, Salavati-Niasari M, Mir N, Kianpour G (2014) Facile synthesis and characterization of nanostructured flower-like copper molybdate by the co-precipitation method. J Cryst Growth 386: 80-87

Shores MP, Bartlett BM, Nocera DG (2005) Spin-frustrated organic-inorganic hybrids of lindgrenite. J Am Chem Soc 127(51): 17986-17987

Swain B, Lee DH, Park JR, Lee CG, Lee KJ, Kim DW, Park KS (2017) Synthesis of $Cu_3(MoO_4)_2(OH)_2$ nanostructures by simple aqueous precipitation: understanding the fundamental chemistry and growth mechanism. Cryst Eng Comm 19(1): 154-165

Vilminot S, André G, Richard-Plouet M, Bourée-Vigneron F, Kurmoo M (2006) Magnetic structure and magnetic properties of synthetic lindgrenite, $Cu_3(OH)_2(MoO_4)_2$. Inorg Chem 45(26): 10938-10946

Xu J, Xue D (2007) Hydrothermal synthesis of lindgrenite with a hollow and prickly sphere-like architecture. J Solid State Chem 180(1): 119-126

Yvon K, Jeitschko W, Parthé E (1977) Lazy Pulverix, a computer program for calculation X-ray and neutron diffraction powder patterns. J Appl Cryst 10: 73-74